Studies in Nonisothermal Rheology: Behavior Near the Glass Transition Temperature and in the Oriented Glassy State

D. A. CAREY, C. J. WUST, Jr., and D. C. BOGUE, *Department of Chemical, Metallurgical and Polymer Engineering, University of Tennessee, Knoxville, Tennessee 37916*

Synopsis

As part of a continuing study of nonisothermal rheology (meaning the simultaneous application of strain and temperature changes), we here consider the behavior of polystyrene near the glass transition temperature T_g. In particular, we measured the increase of the apparent T_g as the cooling rate is increased from 0.003 to 4.5°C/sec. This change (up to 16°C increase) has both practical and theoretical implications. For enhancing the mechanical properties of a glassy product, one desires maximum orientation (stress) just prior to quenching; the optimum deformation/temperature strategy for maximizing stress is affected by the level of T_g. By using a nonisothermal strategy we were able to produce higher frozen-in orientations, and thus higher mechanical properties, than have been previously reported. For a theoretical understanding of the rubbery state just prior to quenching, we used the generalized time–temperature superposition of our prior work; we found that a modified shift factor of the form $a_T(T,T_g^R)$, where T_g^R refers to a rate-dependent T_g, gives an improved fit to data but is not by itself adequate.

INTRODUCTION

Most polymer processing operations involve moving and shaping a polymeric material in the molten state and cooling it rapidly to a solid state. To obtain basic understanding of these processes we have undertaken a series of projects in "nonisothermal rheology," by which is meant response under conditions of simultaneous deformation and temperature change.[1–4] In the present work, we focus on the behavior of polystyrene near the glass transition temperature T_g. Our various objectives are closely related in the context of property enhancement by molecular orientation; that is, significant increases in the glassy modulus and tensile strength can be achieved by rapidly quenching stressed samples from the rubbery state, thereby "freezing in" high levels of molecular orientation. Early work[5–8] and several recent papers[9–12] have followed up various aspects of this problem. It is clear that temperatures not too far above T_g are the best ones for inducing high levels of orientation. At more elevated temperatures the relaxation processes are too fast, and at temperatures very near T_g the sample fails by brittle fracture. One is thus motivated to seek out the best temperature and deformation strategies in a temperature regime somewhat above T_g. One soon encounters the difficulty that T_g itself is affected by the cooling rate (see especially Fox and Flory,[13] Kovacs,[14] Rusch,[15] and Moynihan et al.[16]).

Our studies focus, then, on the nonisothermal rheology near this "moving" T_g and on the properties of the subsequent quenched (glassy) samples. We

Journal of Applied Polymer Science, Vol. 25, 575–588 (1980)

0021-8995/80/0025-0575$01.00

present systematic data with temperature, deformation rate, and cooling rate as the parameters of consideration; the emphasis is on very high cooling rates (up to 4.5°C/sec). We take up the various portions of the work in an order roughly following the chronology of the project: starting with the experimental studies and passing to theoretical studies of the rheology in the rubbery state.

EXPERIMENTAL

The basic experimental apparatus, a modification of that developed by Matsui[1] and Matsumoto,[3] consists of an air oven containing radiant heaters and having also an external blower system which introduces varying mixtures of room air and heated air (see Fig. 1). In the recent modification, Wust[17] developed a control system which automatically introduces a linear cooling rate (or heating rate) by adjusting the relative amounts of room air and heated air. Rates up to 4.5°C/sec were attainable. A small background level of radiant heat was used to smooth out axial temperature variations. The temperature was monitored with a bare thermocouple in the airstream very near the sample. Prior work[3] showed that this thermocouple adequately tracked the (nearly uniform) sample temperature at rates up to 2°C/sec for samples smaller than about 500 μm in diameter. It is possible, however, that we have some temperature gradients in our larger samples at the highest cooling rates. More details of the experimental setup are available in Wust's thesis.[17]

In the work involving the effect of cooling rate on T_g,[17] stationary cylindrical samples (0.5 mm in diameter, 250 mm in length) were clamped in an Instron tensile tester and subjected to cooling rates up to 4.5°C/sec. The force was measured as a function of time.

In the work involving the development of oriented samples,[18] cylindrical rods

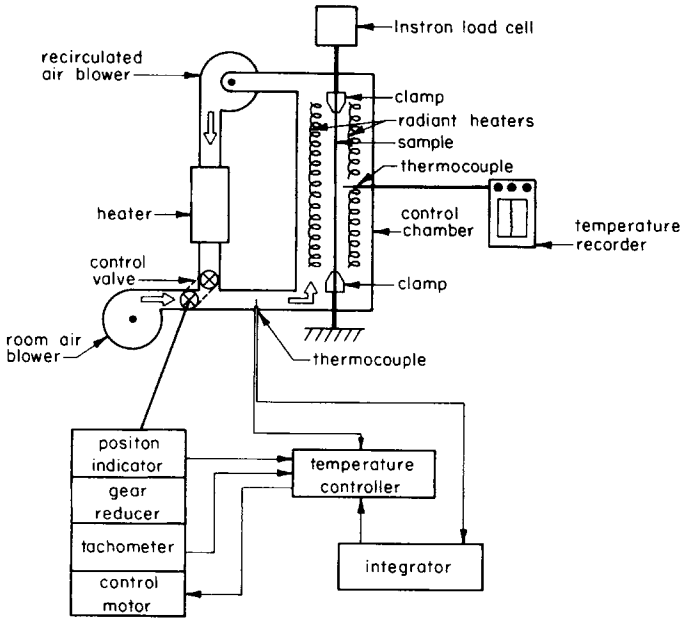

Fig. 1. Schematic diagram of nonisothermal oven and associated control system.

of polystyrene were pulled in two devices: in an Instron tensile tester (as pictured in Fig. 1) and also in a roller-driven device capable of inducing constant elongation rate. In this latter apparatus the sample is held at one end by a clamp connected to an Instron load cell and is pulled at the other end by passing between two rotating rollers.[4] The samples were 500–600 μm in diameter in the nonisothermal runs and 800–900 μm in diameter in the isothermal runs; the initial length varied between 1.5 and 3.0 cm in the Instron apparatus and the length was constant at 13 cm in the roller-driven apparatus. Insofar as possible, we tried to use the roller-driven apparatus, but an experimental difficulty (slippage on the rollers) prevented us from doing so at the lower temperatures (<112°C). Thus, most of the isothermal runs, often involving temperatures below 112°C, were done on the Instron tensile tester. In all parts of the work the original samples were prepared by extrusion from an Instron capillary rheometer and annealed for a few hours at 130°C.

After subjecting the samples to various cooling and pulling histories, they were quenched rapidly by opening doors of the oven and subjected to room air. In a few cases (to be noted later) cold carbon dioxide jets were also directed at the samples in an effort to speed up the quench.

The oriented, quenched samples were subjected to various optical and mechanical tests at room temperature. The birefringence was measured on a Leitz polarizing microscope equipped with a 10-order compensator. Tensile tests (through yielding to fracture) were conducted on an Instron tensile tester. A Rheometrics Inc. Mechanical Spectrometer was used to measure the torsional modulus. Details are available in the thesis by Carey.[18]

The material was a commercial polystyrene (Shell TC 3-30), which has been extensively studied in our earlier work.[1,3,4,19,20] The molecular weight averages are $\overline{M}_n = 6.1 \times 10^4$ and $\overline{M}_w = 28.3 \times 10^4$, giving $\overline{M}_w/\overline{M}_n = 4.6$. Details of the molecular weight distribution and of the rheological properties are available in the prior work.

EFFECT OF COOLING RATE ON GLASS TRANSITION TEMPERATURE

Motivated by our interest in developing highly oriented samples near T_g and by the prior work of Matsumoto and Bogue[3] on the rheology at fast cooling rates, we undertook experiments to measure the value of T_g (or more accurately an apparent T_g) under conditions of fast cooling. Usually, T_g is defined operationally in terms of an abrupt change in the volume coefficient of expansion, an idea which has been generalized to include other derivatives of first-order thermodynamic functions. This view of the glass transition as a second-order transition (see the Ehrenfest equation in ref. 21) has been developed by several workers, notably Davies and Jones,[22] Staverman,[23] and in a more general framework by Christensen.[24] Christensen grapples explicitly with the matter of the time dependence of the various functions and gives a result, similar to the Ehrenfest equation, good for small departures from an equilibrium T_g. We call on these ideas in only a qualitative way because our interest concerns large departures from equilibrium. The effect of cooling rate has been studied experimentally in the papers previously cited[13–16] and theoretically by Saito et al.,[25] who use a first-order rate argument based on free volume. Our emphasis is on

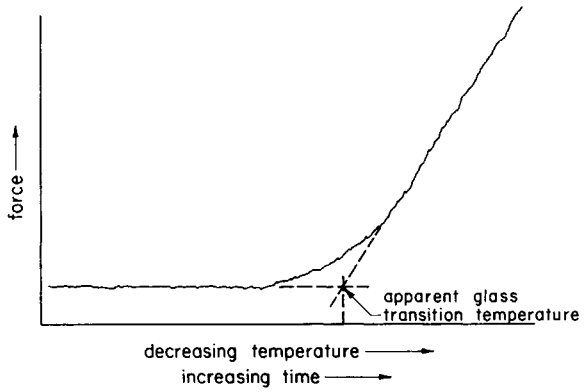

Fig. 2. Typical force–time plot for constrained samples subjected to rapid cooling rates.

quite high cooling rates, up to 4.5°C/sec, compared to rates of the order of degrees per minute in the prior work.

In our experiment we hold a stationary sample between fixed Instron clamps. The temperature is dropped at a controlled linear rate from 140°C to a temperature well below the transition (approximately 70°C). Because of contraction effects, the tensile force on the constrained sample undergoes a sudden change of slope as one passes through a characteristic temperature which we label as an "apparent glass transition temperature" (see Fig. 2). There is a two-step rate process involved here: the temperature change affects the volume, and the volume change affects the force. Roughly following Christensen, we take the view that above T_g, although the volume changes are large, the molecular processes which translate this change to a measurable mechanical stress are relaxing very quickly and practically no change of force is observed. Below T_g the volume changes are smaller and lag behind the temperature but are almost immediately seen as a change in force. We take the crossover point, the appearance of a large force, as an operational definition of T_g under fast cooling conditions.

A plot of the apparent T_g versus cooling rate is shown in Figure 3. Although there is considerable scatter at the higher rates, we found good reproducibility at the lower rates; no points were found below the plotted curve at rates up to

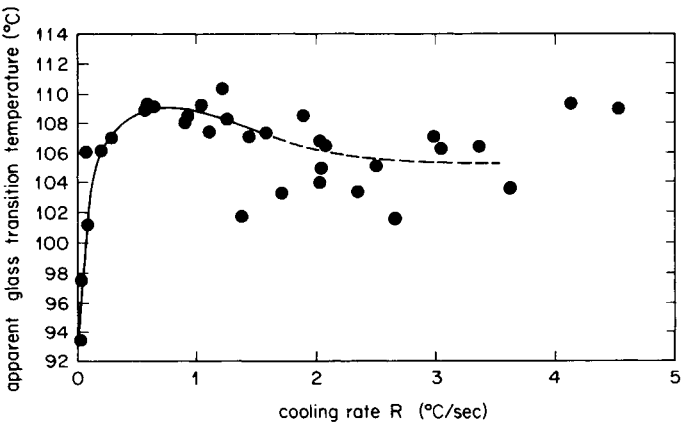

Fig. 3. Apparent glass transition temperature as function of the cooling rate.

1°C/sec. An equilibrium value of 93.5°C (at a cooling rate of 0.003°C/sec) compares with values of 87.5 to 100°C as measured by dilatometry methods.[13,14,26] The scatter at the higher rates may be due to uneven cooling of the samples. In any case, it is clear that there is a substantial increase in T_g (as much as 16°C) with increased cooling rate. Saito et al.[25] predict an increase of about 13°C between cooling rates of 10^{-3} and 1°C/sec and an increase of about 19°C if the upper rate is changed to 10°C/sec. Our results are therefore in reasonable agreement with their predictions although their theory does not predict the flattening out suggested by the data of Figure 3. We make use of our experimental results in the subsequent sections.

DEFORMATION/TEMPERATURE STRATEGIES FOR PRODUCING HIGHLY ORIENTED SAMPLES; MECHANICAL PROPERTIES

From physical considerations one supposes that there are optimum thermal and elongation conditions for producing highly oriented samples. At higher temperatures (or lower pulling rates) the molecules relax too quickly to provide substantial orientation, and at lower temperatures (or higher pulling rates) they behave in a glassy manner and fracture at very small elongations. We present systematic data in terms of these two variables in Figure 4. We found optimum conditions at 105°C, at initial elongation rates ($\dot{E} = (1/L)dL/dt$ at time zero) in the range of about 0.28 to 0.56 sec^{-1} (cross-head speeds in the range 50–100 cm/min for the 3.0-cm samples used).

In view of our interest in nonisothermal processes, we then explored various combinations of cooling rates and elongation rates. (The apparatus was the roller take-up device, allowing imposition of constant $\dot{E}$.) The general strategy is shown in Figure 5 with the initial temperature being in the range 130–150°C. It was quickly found that terminating at 105°C, followed by continued pulling there resulted in a cloudy, crazelike appearance. We interpreted this as glassy-like behavior; i.e., at finite cooling rates, T_g is raised substantially, as can be seen in Figure 3. In the subsequent runs, the strategy was one of timing the

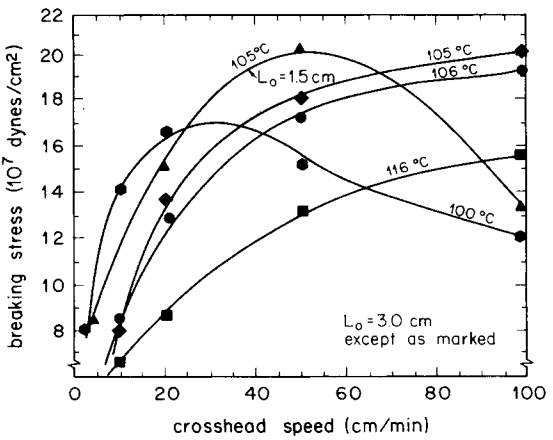

Fig. 4. True breaking stress under isothermal conditions just above T_g, at various pulling rates.

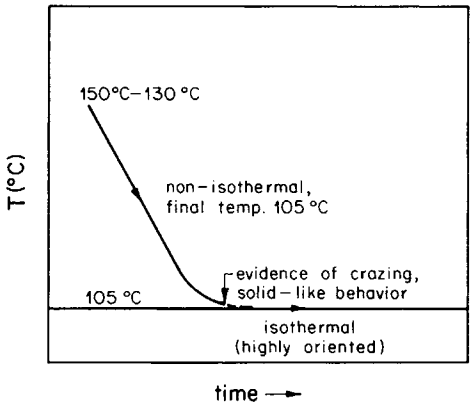

Fig. 5. Temperature strategies used during nonisothermal runs.

cooling and stretching histories so that the temperature was just short of incipient cloudiness (crazing) and the deformation was just short of that to cause breakage. (In a few cases, the experiments were carried to the break point to determine the limiting conditions.) These data are summarized in Figure 6.

It is clear that we were able to achieve substantially higher stresses under the nonisothermal conditions. However, in many cases (points in the area marked "samples relaxed") we were not able to extract these samples from the oven in their highly stressed state. Even with the introduction of cold CO_2 jets, we could not freeze in the stress that was achieved; this was noted directly as a decrease on the Instron force plot and indirectly as a lower-than-expected birefringence in the subsequent samples. We interpret this behavior as glassy response. At these high cooling rates, also possibly affected by the stress level itself, the material is below its effective T_g, and some of the observed stress is caused by an "unlocking" of rigid molecules (the glassy mechanism probably associated with a volume change) and some of the stress is caused by an orientation of the molecules (the rubbery mechanism). Where samples could be quenched and with-

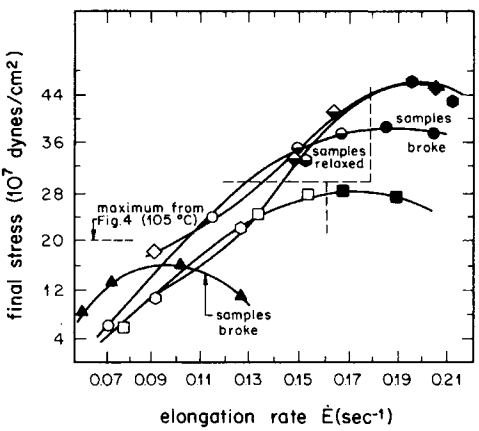

Fig. 6. True breaking (or final) stress under nonisothermal conditions, at various constant elongation rates (open symbols, usable samples produced; half symbols, samples relaxed; solid symbols, samples broke): ▲, 112°C, R = 0 (isothermal); ■□, 140°C, R = 2.5°C/sec; ◆◆◇, 140°C, R = 4.5°C/sec; ◒●○, 130°C, R = 4.5°C/sec; ◒●○, 150°C, R = 4.5°C/sec.

drawn, we were able to achieve stresses about 40% higher in the nonisothermal runs than in the best isothermal runs. We attribute this in some very rough way to an enhanced "massaging out" of microdefects which eventually lead to cohesive failure; lower temperatures are necessary to get high orientations but higher temperatures are necessary to eliminate points of incipient failure.

Finally then, the quenched samples were removed for room temperature measurement of the optical and mechanical properties (Figs. 7–11). Figure 7 shows a plot of the frozen-in orientation (as measured by birefringence) as a function of the true stress in the rubbery samples (as calculated from the force on the Instron load cell during the quench). These results are in good agreement with the prior work of Matsumoto and Bogue,[4] who did simultaneous (on-line) measurements of birefringence and stress, and with Oda, White, and Clark,[27] who did both on-line and off-line measurement of birefringence. While a case might be made for a systematic difference at stresses above 10^8 dyn/cm^2, we feel that, within the scatter, one can consider the stress–birefringence relationship to be a general one, independent of how the sample is oriented or when the birefringence is measured.

Subsequent figures summarize the mechanical properties, with Figure 8 showing typical stress–strain curves. The stress shown is the engineering stress (i.e., the force divided by the original cross-sectional area of the sample). In agreement with Tanabe and Kanetsuna,[12] we find that a small amount of orientation (birefringence) results in an enormous change in the ductility, inducing a brittle to ductile transition at values as low as $|\Delta n| = 2 \times 10^{-3}$. Tanabe and Kanetsuna[28] report accompanying wide-angle x-ray scattering measurements and associate this transition with a tendency for the phenyl rings to orient perpendicular to the chain direction and to "slide together" with rings from adjacent molecules. This increased ductility shows itself markedly in Figure 9 (elongation-to-break vs. birefringence). As expected, the elastic moduli (Young's modulus and the torsional modulus) increase with increasing birefringence (Figs. 10 and 11). Somewhat surprisingly, the material appears to be relatively isotropic in these two properties; that is, the ratio of the Young's modulus to the torsional modulus is essentially 3 over the entire range. The tensile strength

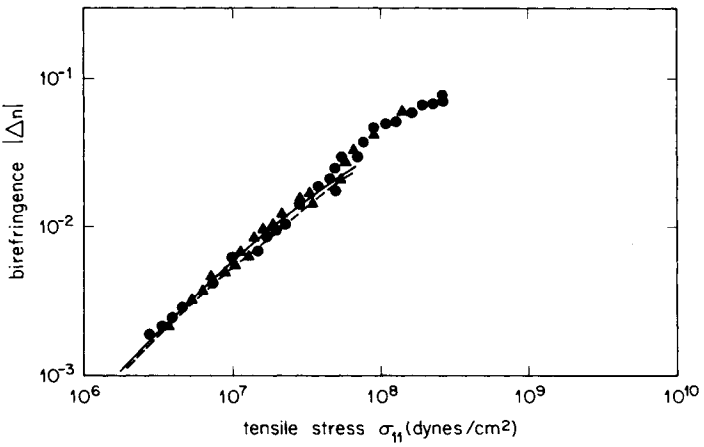

Fig. 7. Summary of true stress–birefringence data: (▲) isothermal, this work; (●) nonisothermal, this work; (—) Matsumoto and Bogue; (- - -) Oda, White, and Clark.

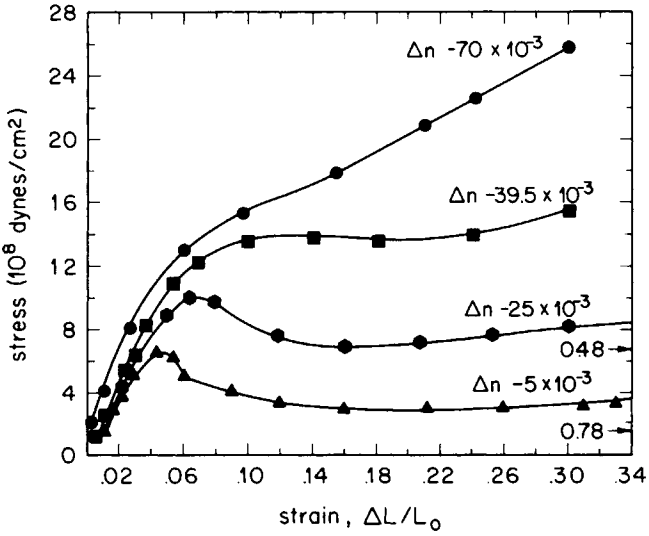

Fig. 8. Typical stress–strain curves for oriented, glassy samples (engineering stress).

(Fig. 11) and the yield strength (not shown but deducible from Fig. 8) also increase substantially with increasing birefringence. In all of these figures the words "isothermal" and "nonisothermal" refer to the conditions under which the oriented samples were prepared; the mechanical tests themselves were conducted at room temperature. Our nonisothermally produced birefringences ($|\Delta n| \approx 7.5 \times 10^{-2}$) are comparable to those reported earlier by our group using a melt spinning technique[29]; these birefringences (orientations) are higher than values reported elsewhere. Prior values were mostly in the range (1.5–2.0) $\times$ 10^{-2}, with Tanabe and Kanetsuna's data[12] going to 3.2×10^{-2}.

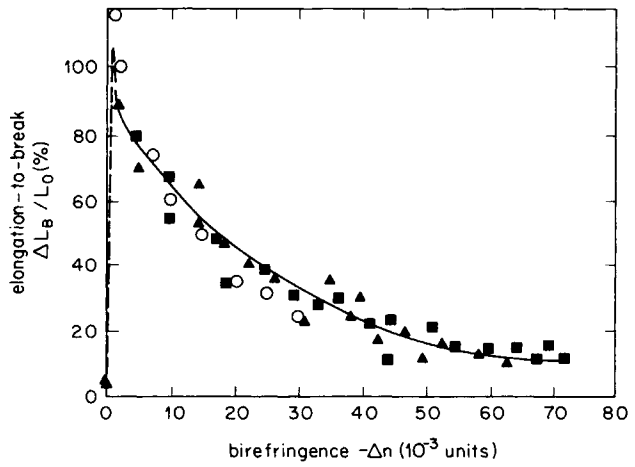

Fig. 9. Elongation-to-break as function of birefringence at room temperature; ■, nonisothermal, ▲, isothermal, present data ($\dot{E}_0 = 0.017$ sec^{-1}); ○, Tanabe–Kanetsuna data.

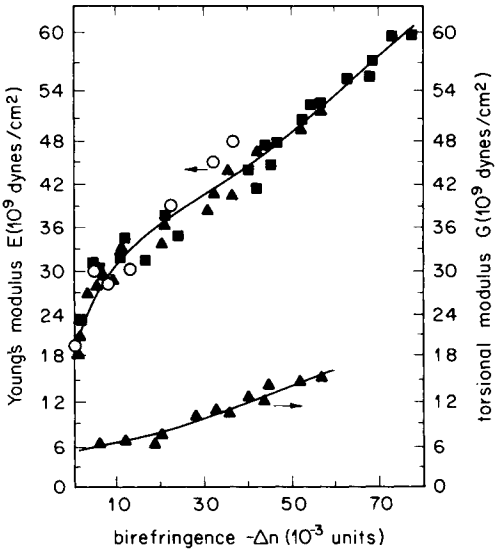

Fig. 10. Young's modulus and torsional modulus as function of birefringence at room temperature; ■, nonisothermal, ▲, isothermal, present data ($\dot{E}_0 = 0.017$ sec^{-1}); ○, Tanabe-Kanetsuna data.

THEORETICAL ANALYSIS OF STRESS DEVELOPMENT ABOVE THE GLASS TRANSITION TEMPERATURE

Using the nonisothermal viscoelastic theory we have previously proposed,[1,3] it should be possible to predict the development of stress in the rubbery state, prior to quenching. In view of the generality of the stress–birefringence law for amorphous melts and solutions,[4,27] this allows us also to predict the development of birefringence or orientation. Oda, White, and Clark[27] discuss the connections among stress, birefringence, and orientation in some detail. As stated originally,

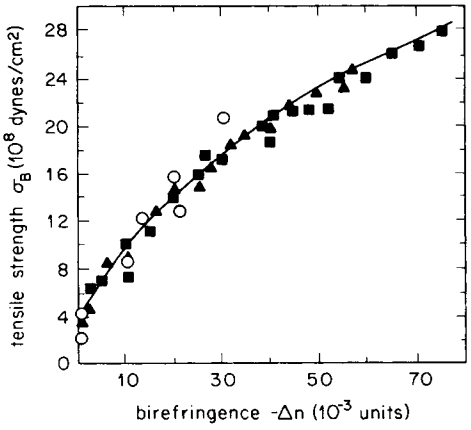

Fig. 11. Tensile strength as function of birefringence (engineering stress) at room temperature; ■, nonisothermal, ▲, isothermal, present data ($\dot{E}_0 = 0.017$ sec^{-1}); ○, Tanabe-Kanetsuna data.

the viscoelastic theory for stress is of the form[1]

$$\sigma_{ij}(t) = -p\delta_{ij} + \sum_n G_n^0 \int_{-\infty}^{t} \frac{\exp\left[-\int_{t'}^{t} \frac{dt''}{\tau_n(t'')}\right]}{\tau_n(t')} c_{ij}^{-1}(t,t')\, dt' \tag{1}$$

where σ_{ij} is the total stress; p is the negative of the isotropic stress; G_n^0 and τ_n are elastic moduli and time constants, respectively (here assumed constant with no deformation rate dependence); c_{ij}^{-1} is the relative Finger strain tensor; t is the present time; and t' is an arbitrary past time (the variable of integration). We omit here the dependence of G_n^0 on temperature, assigning the major temperature effects to the temperature dependence of τ_n, which is treated with a shift factor a_T of the form

$$\tau_n(t') = a_T[T(t')]\tau_n^0 \qquad \tau_n(t'') = a_T[T(t'')]\tau_n^0 \tag{2}$$

where τ_n^0 is the time constant at the reference temperature, corresponding to $a_T = 1$. We also stated a deformation-dependent ("nonlinear") equation for τ_n, the so-called Bogue–White model, but we do not use that here. Recently, Dietz and Bogue,[30] amplifying the remarks of Matsui and Bogue[1] about the shortcomings of eq. (1) in certain transient flows, have presented a more complicated form [eq. (1) does not, for example, predict stress overshoot in shear flow]. Since we are using a linear formulation here (G_n^0, τ_n^0 constant), these complications can be avoided. Finally, the relationship between our formulation and that used by Fisher and Denn[31] is now better understood (see Appendix).

As a conceptual matter we note that while eq. (1) is a generalization of the usual time–temperature superposition, it is not a completely straightforward generalization. That is, if we consider some instant of time t' in the past, the amount of relaxation between then (t') and now (t) depends not just on the temperature then but rather on the complete history between then and now. Thus, a second integration, using the time index t'', is required.

The shift factor a_T is usually presented in terms of the Williams, Landel, and Ferry (WLF) equation,[32] stated here using the equilibrium glass transition temperature T_g^0 as the reference temperature:

$$\log a_T^0 = \frac{-C_1(T - T_g^0)}{C_2 + T - T_g^0} \tag{3}$$

Matsumoto and Bogue[3] noted that at fast cooling rates near the glass transition, one gets a better fit to the data using a cooling rate-dependent T_g, designated T_g^R. The corresponding shift factor a_T^R is obtained by replacing T_g^0 in eq. (3) with T_g^R.

In setting up the mathematical formulation, it proves convenient to use a new reference temperature, one identical to the initial temperature of the sample. Designating this reference temperature by T^*, we write

$$\log a_T{}^{0,*} = \frac{-C_1C_2(T - T^*)}{(C_2 + T^* - T_g^0)(C_2 + T - T_g^0)} \tag{4}$$

which is similar for $a_T{}^{R,*}$, where T_g^0 is replaced by T_g^R. A great mathematical simplification results if we approximate eq. (4) by

$$\ln a_T{}^{0,*} = -\alpha_{0,*}(T - T^*) \tag{5a}$$

or

$$\ln a_T^{R,*} = -\alpha_{R,*}(T - T^*) \tag{5b}$$

where the slope depends on the T_g selected and also on the reference temperature selected. Figure 12 shows that eq. (5) gives a reasonable approximation to the shift factor over the range of interest. The data in Figure 12 are taken from Takaki[33] and can be fit by a WLF equation, eq. (4), using $C_1 = 15.5$, $C_2 = 45.5°C$, and $T_g^0 = 94°C$ (the latter from Fig. 3). Using Eq. (5a) and a natural logarithm coordinate gives $\alpha_{0,*} = 0.25°C^{-1}$ for the straight line.

Finally then, the stress development during constant $\dot{E}$ pulling ($[c_{11}^{-1} = \exp[2\dot{E}(t - t')]$, $c_{22}^{-1} = c_{33}^{-1} = \exp[-\dot{E}(t - t')]$), upon which is superposed a linear cooling rate $R[T(t) = T^* - Rt]$, can be stated by

$$\sigma_{11}(t) = \sum_n G_n^0 \dot{E} \int_0^t \exp\left[\frac{\exp(-\alpha_{0,*}Rt) - \exp[-\alpha_{0,*}R(t-s)]}{\alpha_{0,*}R\tau_n(*)}\right] \times [2\exp(2\dot{E}s) + \exp(-\dot{E}s)\, ds] \tag{6}$$

where $s = t - t'$ and where $\tau_n(*)$ means τ_n evaluated at T^*. This result has been presented by Matsui and Bogue.[2] A restatement is made in the recent thesis by Carey.[18]

We present the theoretical predictions of eq. (6) in Figures 13 and 14. A six-element model (six G_n^0 and six τ_n^0) was used, with the values being those given by Matsui and Bogue[1] at 137°C, adjusted to the appropriate reference temperature T^*. These 12 constants are being obtained from independent experiments, and thus there are no adjustable parameters in the present analysis. The dotted lines show the original Matsui–Bogue theory, that is, $\alpha_{0,*}$ (based on T_g^0), whereas the solid lines present the Matsumoto–Bogue modification, that is, $\alpha_{R,*}$ (based on T_g^R). Values of T_g^R are estimated from Figure 3. Clearly, using the rate-dependent glass transition temperature helps the fit of data to theory, giving a quite satisfactory fit at 2.5°C/sec but only a move in the right direction at 4.5°C/sec. Note that a number of the points in disagreement are hotter than the rate-adjusted transition temperature T_g^R (we would certainly expect disagreement below T_g^R). Because the data are higher than the theoretical curves, it seems clear then that a glassy mechanism must be coming into play above T_g^R when the material is cooled quite rapidly. Simply adjusting our reference point, that is, $T_g^0 \rightarrow T_g^R$, in the manner of Matsumoto and Bogue is not adequate at the

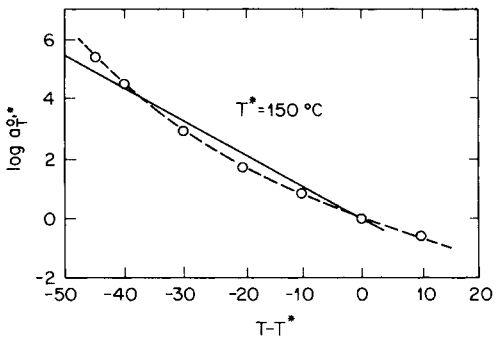

Fig. 12. Time–temperature shift factor a_T. Data and WLF equation, compared to simplified equation.

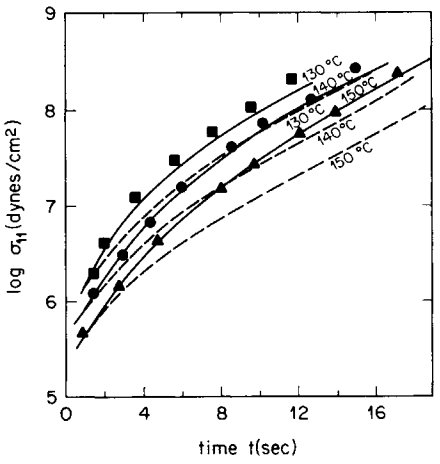

Fig. 13. Theoretical prediction of true stress development in the rubbery state at a moderate cooling rate: original and modified (rate-dependent T_g) theories, $R = 2.5°C/sec$; $\dot{E} = 0.12\ sec^{-1}$; (▲) $T_0 = 150°C$; (●) $T_0 = 140°C$; (■) $T_0 = 130°C$; (—) theory $\tau = \tau(T,R)$; (- - -) theory $\tau = \tau(T)$.

higher rates. We feel that the introduction of completely new time constants, somehow related to the glassy state, must be introduced, although how they will be stated in terms of T (or dT/dt) is not presently clear.

MAJOR CONCLUSIONS

Fast cooling rates have a significant effect on the apparent glass transition temperature T_g, as determined from the force created by the volume contraction of a clamped sample. For polystyrene the T_g so measured is 12–16°C higher than the equilibrium value for cooling rates in the range 0.5–4.5°C/sec. This fact has both theoretical and practical implications in the processing of amorphous polymers.

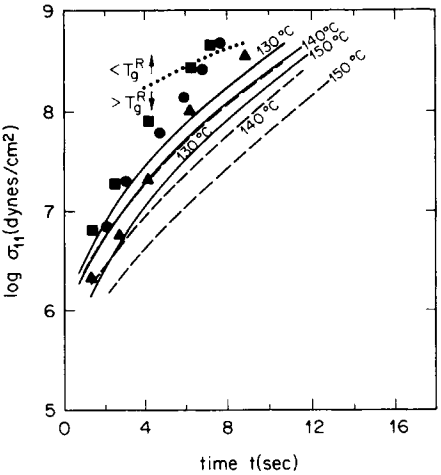

Fig. 14. Theoretical prediction of true stress development in the rubbery state at a high cooling rate: original and modified (rate-dependent T_g) theories, $R = 4.5°C/sec$; $\dot{E} = 0.19\ sec^{-1}$; (▲) $T_0 = 150°C$; (●) $T_0 = 140°C$; (■) $T_0 = 130°C$; (—) theory $\tau = \tau\ (T,R)$; (- - -) theory $\tau = \tau\ (T)$; (. . .) locus of passage through T_g^R.

In terms of a theoretical understanding of the rheological behavior of a rubbery melt being simultaneously cooled and deformed, the shift of T_g with cooling rate is the symptom of a loss of mobility (or start of glassy-like behavior) at temperatures well above the normal rubbery–glassy transition. A generalized (integral) time–temperature superposition for the rubbery state can be stated which correlates a great deal of stress growth data, provided that the T_g which appears in the shift factor equation (the WLF equation) is made cooling rate dependent. In notational form, rubbery time constants τ of the form $\tau[a_T(T,T_{g'}^R)]$ are a substantial improvement over those of the form $\tau[a_T(T,T_g^0)]$, although even the former is not adequate when the cooling rate is very high (4.5°C/sec). We feel that a completely satisfactory theory must involve the introduction of completely new time constants, somehow associated with a glassy state mechanism.

In terms of preparing highly oriented samples, nonisothermal (cooling) deformations in the rubbery state must be carried out at higher final temperatures than isothermal deformations. Otherwise, glassy (crazelike) imperfections appear. Nonisothermal histories have the advantage of permitting higher stresses (orientations) in the rubbery state before breakage occurs, although the mechanism is not very clear. We are able to create orientations comparable to our prior melt spinning work[29] and higher than values reported elsewhere.

Finally, the mechanical properties of the oriented glassy product correlate quite well with the orientation (birefringence) frozen into it, which in turn correlates quite well with the stress induced in the melt at the time of quenching. This is true whether or not the melt history is isothermal or nonisothermal. Young's modulus, the torsional modulus, the tensile strength, and the yield strength (when a yield is present) all increase with increasing orientation. The elongation-to-break increases enormously with the introduction of only a very small amount of orientation and then decreases with further increases of orientation. This induction of a brittle-to-ductile transition at very low orientations is in agreement with the recent results of Tanabe and Kanetsuna.[12,28]

The authors acknowledge with thanks the help of the National Science Foundation which provided general financial support for the project and a research fellowship for C.J.W. (under Grant No. ENG 76-15644) and the help of the Plastics Institute of America which provided a research assistantship for D.A.C.

Appendix: Connection Between Differential and Integral Forms of Nonisothermal Viscoelastic Theory

Our nonisothermal theory has an integral form, eq. (1), whereas Fisher and Denn[31] use a differential form in their analysis of melt spinning. These are related to each other as can be shown easily for the case of a one-dimensional (nontensor), simple Maxwell (one relaxation time) statement of the theory. The purpose here is to show that connection. The more general relationship—between our general form and Fisher and Denn's general form [their eq. (1)]—has not been worked out.

The one-dimensional, one-element differential Maxwell theory for nonisothermal flows is

$$\sigma + \tau(t)\frac{d\sigma}{dt} = G\,\tau(t)\,\dot{\gamma} \tag{A1}$$

where $\tau(t)$ is shorthand notation for $\tau[T(t)]$; that is, the temperature depends on the time and the time constant depends on the temperature. We first presume and then show that the following is a general solution to eq. (A1):

$$\sigma = G\int_{-\infty}^{t} \exp\left[-\int_{t'}^{t}\frac{dt''}{\tau(t'')}\right]\dot{\gamma}(t')\,dt' \tag{A2}$$

An integration by parts, with the requirement that the relative strain tensor $\gamma = 0$ at $t' = t$, gives

$$\sigma = -G \int_{-\infty}^{t} \exp\left[-\int_{t'}^{t} \frac{dt''}{\tau(t'')}\right] \frac{\gamma(t,t')}{\tau(t')}\, dt' \tag{A3}$$

Equation (A1) is the simple Maxwell analog of Fisher and Denn's general form, and eq. (A3) is the analog of our general form, eq. (1).

Now eq. (A2) is a solution to eq. (A1). This can be demonstrated by differentiating eq. (A2), using Leibnitz's rule, and simplifying:

$$\frac{d\sigma}{dt} = G\,\dot{\gamma}(t) + G \int_{-\infty}^{t} \left\{\exp\left[-\int_{t'}^{t} \frac{dt''}{\tau(t'')}\right]\right\} \left\{\frac{-1}{\tau(t)}\right\} \dot{\gamma}(t')\, dt' \tag{A4}$$

Substituting eqs. (A2) and (A4) into eq. (A1) yields an identity, as required.

References

1. M. Matsui and D. C. Bogue, *Trans. Soc. Rheol.*, **21**, 133 (1977); M. Matsui, M.S. Thesis, University of Tennessee, Knoxville, 1976.
2. M. Matsui and D. C. Bogue, *Polym. Eng. Sci.*, **16**, 735 (1976).
3. T. Matsumoto and D. C. Bogue, *Trans. Soc. Rheol.*, **21**, 453 (1977).
4. T. Matsumoto and D. C. Bogue, *J. Polym. Sci., Polym. Phys. Ed.*, **15**, 1663 (1977).
5. L. E. Nielsen and R. Buchdahl, *J. Appl. Phys.*, **21**, 488 (1950).
6. R. G. Cheatham and A. G. H. Dietz, *Mod. Plast.*, **29**, 113 (September, 1951).
7. K. J. Cleereman, H. J. Karam, and J. L. Williams, *Mod. Plast.*, **30**, 119 (September, 1953).
8. G. B. Jackson and R. L. Ballman, *SPE J.*, **16**, 1147 (1960).
9. J. Hennig, *J. Polym. Sci. Part C*, **16**, 2751 (1967).
10. L. S. Thomas and K. J. Cleereman, *SPE J.*, **28**, 61 (1972).
11. T. T. Jones, *Pure Appl. Chem.*, **45**, 39 (1976).
12. Y. Tanabe and H. Kanetsuna, *J. Appl. Polym. Sci.*, **22**, 2707 (1978).
13. T. G. Fox and P. J. Flory, *J. Appl. Phys.*, **21**, 581 (1950).
14. A. J. Kovacs, *J. Polym. Sci.*, **30**, 131 (1958).
15. K. C. Rusch, *J. Macromol. Sci., Phys.*, **2**, 179 (1968).
16. C. T. Moynihan, P. B. Macedo, C. J. Montrose, P. K. Gupta, M. A. DeBolt, J. F. Dill, B. E. Dom, P. W. Drake, A. J. Easteal, P. B. Elterman, R. P. Moeller, H. Sasabe, and J. A. Wilder, *Ann. N. Y. Acad. Sci.*, **279**, 15 (1976).
17. C. J. Wust, Jr., M.S. Thesis, University of Tennessee, Knoxville, 1978.
18. D. A. Carey, M.S. Thesis, University of Tennessee, Knoxville, 1979.
19. T. Takaki and D. C. Bogue, *J. Appl. Polym. Sci.*, **19**, 419 (1975).
20. R. Racin and D. C. Bogue, *J. Rheol.*, **23**, 263 (1979).
21. I. Prigogine and R. Defay, *Chemical Thermodynamics*, Longmans, Green, London, 1954.
22. R. O. Davies and G. O. Jones, *Adv. Phys.*, **2**, 370 (1953).
23. A. J. Staverman, *Rheol. Acta*, **5**, 283 (1966).
24. R. M. Christensen, *Trans. Soc. Rheol.*, **21**, 163 (1977).
25. N. Saito, K. Okano, S. Iwayanagi, and T. Hideshima, in *Solid State Physics: Advances in Research and Applications*, Vol. 14, Academic, New York, 1963.
26. G. Menges and P. Thienel, *Kunststoffe*, **65**, 696 (1975).
27. K. Oda, J. L. White, and E. S. Clark, *Polym. Eng. Sci.*, **18**, 53 (1978).
28. Y. Tanabe and H. Kanetsuna, *J. Appl. Polym. Sci.*, **22**, 1619 (1978).
29. T. Matsumoto and D. C. Bogue, *Polym. Eng. Sci.*, **18**, 564 (1977).
30. W. Dietz and D. C. Bogue, *Rheol. Acta*, **17**, 595 (1978).
31. R. J. Fisher and M. M. Denn, *AIChE J.*, **23**, 23 (1977).
32. J. D. Ferry, *Viscoelastic Properties of Polymers*, 2nd ed., Wiley, New York, 1970.
33. T. Takaki, M.S. Thesis, University of Tennessee, Knoxville, 1973.

Received August 1, 1979
Revised September 24, 1979